UvA-DARE (Digital Academic Repository)

Independent mode sorption of perfluoroalkyl acids by single and multiple adsorbents

Krop, H.; Eschauzier, C.; van der Roest, E.; Parsons, J.R.; de Voogt, P.

Link to publication

Citation for published version (APA):
Krop, H., Eschauzier, C., van der Roest, E., Parsons, J. R., & de Voogt, P. (2021).
Independent mode sorption of perfluoroalkyl acids by single and multiple adsorbents.
Environmental Science Processes & Impacts, *23*(12), 1997-2006.
https://doi.org/10.1039/d1em00322d

PAPER

Independent mode sorption of perfluoroalkyl acids by single and multiple adsorbents†

Hildo Krop, [ID] *[a] Christian Eschauzier,[b] Els van der Roest,[d] John R. Parsons[c] and Pim de Voogt [ID] [cd]

Infinite dilution partition coefficients, $K_{p,0}$, of a series of unbranched perfluoralkylacids, PFAAs with 3 to 8 CF_2 units between water and commercially available weak anion exchange (WAX) and strong anion exchange (MAX) polymers, C_{18}-modified silica, hydrophilic–lipophilic balance polymer (HLB), and Al_2O_3 sorbents were determined with self-packed columns using an HPLC-MS/MS setup. The anionic WAX sorbent shows a much higher adsorption affinity (about 450 fold) for PFBA than was observed for the applied hydrophobic sorbent HLB. Since the incremental value for each CF_2 group is smaller when the electrostatic adsorption process is observed, the hydrophobic partition coefficient of HLB supersedes the electrostatic one of WAX at around PFTeDA. Adsorption of PFAAs to Al_2O_3 was weak and did not show a clear chain length dependency. A recently developed independent mode (IM) adsorption model is a more accurate model to combine the electrostatic and hydrophobic interaction terms. This model predicts the correct behaviour of especially short chain PFAAs in soil or sediment sorption experiments. Factors increasing sorption efficiency of well- and ill-defined single and multiple adsorbents towards PFAAs are discussed. The IM model provides a method to optimise sorption remediation strategies of PFAAs in contaminated waters and proposes a two-step strategy, a starting hydrophobic step followed by an electrostatic one to remove more efficiently the short chain PFAAs.

Environmental significance

This paper addresses sorption of a range of PFAAs ($N_{CF_2} = 3–15$) onto five specifically selected sorbents. The results of the individual sorption processes are interpreted by a recently developed Independent Mode model by the same authors. This model distinguishes clearly why sorption processes of PFAAs to different adsorbents needs to be modelled by addition of the specific partition coefficients, K_p (L kg^{-1}) of the hydrophobic and electrostatic sorption process, rather than by addition of their specific standard Gibbs energies, $\Delta_s G^0$ (kJ mol^{-1}). The highest sorption efficiency is achieved by searching for adsorbents which combine a high sorption constant, K_L (L $mmol^{-1}$), and high number of sorption location, C_s^{max} (mmol kg^{-1}) for both the hydrophobic and electrostatic interaction. The IM-model also concludes that a two-step adsorption technology, a hydrophobic one followed by an electrostatic one is more efficient than mixing such type of adsorbents together. Therefore this paper establishes a methodology to improve sorption remediation technologies for PFAAs.

1. Introduction

Perfluoroalkyl acids (PFAAs) are surfactants composed of a completely fluorinated alkyl chain (tail) and a carboxylic functional head[1] group, which are deprotonated at environmentally relevant pH values[2,3] and their hydrophobicity increases with increasing fluorocarbon chain length.[4] PFAAs have been found to be very persistent in humans and the environment and are globally present in all kinds of environmental matrices such as biota, air and surface waters.[5,6] This has lead to global concern and to initiatives to restrict the use of PFAAs in for example fire fighting foams in the EU.[7]

Drinking water and food intake are major contributors to human exposure to PFAAs.[8–10] The presence of PFAAs in drinking water is therefore regarded as undesirable. It has led to many reviews addressing both chemical and physical remediation technologies of drinking water production processes.[11–13] Despite these different technologies adsorption by natural systems or man-made systems especially based on granulated activated carbon (GAC), are applied predominantly.[14,15] However, the use of GAC has the disadvantage that PFAAs with shorter chain length $C < 6$ are adsorbed less efficiently. This has stimulated the search for adsorbents which also more efficiently remove PFAAs with short chain lengths. It has been shown that hydrophobic interactions of the tail governs adsorption of

[a]Krop-Consult, Conradstraat 7, 1505 KA Zaandam, The Netherlands. E-mail: hkrop@outlook.com

[b]Christian Eschauzier, Trouringhstraat, 18-1, 1055 HB Amsterdam, The Netherlands

[c]Institute for Biodiversity and Ecosystem Dynamics, University of Amsterdam, Science Park 904, 1098 XH Amsterdam, Netherlands

[d]KWR Water Research Institute, P.O. Box 1072, 3430 BB Nieuwegein, Netherlands

This journal is © The Royal Society of Chemistry 2021

Environ. Sci.: Processes Impacts, 2021, **23**, 1997–2006 | 1997

PFAAs to carbon containing materials like GAC, powdered activated carbon, and carbon nanotubes while anionic interactions govern adsorption to anion-exchange resins (AER) like mixed-mode, strong Anion-eXchang (MAX), Weak Anion-eXchange (WAX), different kinds of clay mineral and metal oxides like several aluminium and iron oxides.[16–23] Special treatments of these adsorbents or changing the pH or ionic strength of the solution can also change the sorption strength in varying degree. In addition adsorption strength also increases on increasing carbon chain length with both types of sorption interaction. It appears that the electrostatic interaction is more often dominant for shorter chain PFAAs while the hydrophobic interaction dominates longer chain PFAAs.[24] Reported soil or sediment properties that specifically govern sorption processes of PFAAs are soil organic carbon fraction,[25,26] protein content and anionic exchange capacity (AEC).[27] Despite many attempts modelling and understanding adsorption behaviour of surfactants in general and PFAAs in particular remains difficult. Both linear and more often non-linear models like the Langmuir and Freundlich isotherms have been applied with limited success in that they could explain the observed phenomena but could not extrapolate the model to other similar reported sorption phenomena.[28,29] Models that incorporate a hydrophobic, electrostatic and/or other sorption energy term on the same sorption location are called dual-mode models (DM) *e.g.* the Donnan and Virial models applied to PFAA.[27,30,31] However in a recent paper[32] this DM interaction model has been compared to an independent mode (IM) model where both interaction terms on different sorption locations are considered. This IM model could not only derive the thermodynamic equations governing the DM model under specific conditions, but could also explain other sorption phenomena such as fast and slow desorption, mixed first and second order rate processes and kinetic hysteresis.

The present study reports on the adsorption affinity of a series of six unbranched PFAAs with 3 to 8 CF_2 units ($N_{CF2} = 3$–8) to five different sorbents including commercially available anionic (anion-exchange) and hydrophobic materials. The measured data are interpreted in order to understand how more efficient adsorption materials for PFAAs can be selected. We show how these individual adsorption materials can be combined to estimate the sorption efficiency of PFAAs in simple batch experiments.

2. Materials and methods

2.1 Chemicals and materials used

Methanol (ULC/MS, Biosolve, Valkenswaard, The Netherlands); sub-boiled water (in-house produced); ammonium acetate (99.999%, Sigma Aldrich, Zwijndrecht, The Netherlands) were used for liquid chromatography. The chemicals injected were: perfluorobutanoic acid (PFBA), perfluoropentanoic acid (PFPeA), perfluorohexanoic acid (PFHxA), perfluoroheptanoic acid (PFHpA), perfluorooctanoic acid (PFOA) and perfluorononanoic acid (PFNA) and were supplied by Sigma Aldrich. Sorbents used were: WAX, HLB and MAX (Waters, Etten-Leur, The Netherlands); Al_2O_3 (0.063–0.200 mm, Merck, Darmstadt, Germany); silicium carbide (SiC, Alfa Aesar, Germany) and C_{18} as a commercially available column (Pathfinder 300 PS; internal diameter 4.6 mm; length 50 mm; particle diameter 3.5 μm; Shimadzu, Duisburg, Germany).

2.2 Column preparation

The C_{18} column was the only commercially available column that was used and consisted of a Si-network with chemically bonded C18-groups. Other sorbent materials were not available as commercial columns, and were either packed from powdered material or from particles obtained from dismantled SPE cartridges. Stainless steel HPLC columns (10 × 2 mm) were filled with either HLB; WAX; MAX or Al_2O_3. In the case of the WAX and MAX materials, columns were filled with a 1 : 99 ($w : w$) mixture of WAX or MAX and SiC. Table 1 shows an overview of the different properties of the adsorbents.

Columns were weighed before and after filling to measure the exact amount of material added. The inertness of SiC was checked by injecting PFBA and PFOA and observing no retention of the analytes, that eluted with the void peak corresponding to the dead volume of the column. All materials had

Table 1 Relevant properties of the sorbents tested. Information from packaging or contact with manufacturer if not stated otherwise

Name	Surf. area	Particle size	Pore size	Anion exchange capacity (AEC)	Estimated number of sorption sites[a]	
Unit	$m^2\ g^{-1}$	μm	Å (angstrom)	μmol m^{-2}	mmol kg^{-1}	Polarity
WAX	800	30	80	0.723	578	Electrostatic (positive)
C_{18}	73[b]	3	100	ne[f]		Hydrophobic
HLB	800	30	80	ne	261[e]	Hydrophobic
Al_2O_3	15[c]	60–75[d]		0.0700[c]	0.10	Electrostatic (positive)
MAX	815	30	80	0.301	245	Electrostatic (positive)
SiC				ne		Inert

[a] Can be found from literature or calculated by multiplying surface area by AEC value for anionic interaction as is done here. [b] Confirmed by in-house Brunauer–Emmet–Teller (BET) measurements. [c] Schwarzenbach *et al.* (2016).[34] [d] Done by fractioning with 60–75 μm sieves. [e] Bäuerlein *et al.* (2012).[33] [f] ne = non-existent.

1998 | *Environ. Sci.: Processes Impacts*, 2021, **23**, 1997–2006

This journal is © The Royal Society of Chemistry 2021

a particle size in the same order of magnitude: 30–75 μm, except for C_{18} (3.5 μm), which may be important for the adsorption process. Columns were conditioned prior to use during 2 h with a 60 : 40 MeOH : H_2O flow of 0.2 mL min^{-1}. Column temperatures were maintained at 30 °C in a column oven.

2.3 Experimental procedure

Solutions in methanol were made for each compound with a concentration range of 5.0–503 ng ml^{-1} (8 levels) and were stored at −20 °C to prevent any evaporation of methanol. Before injection, the methanol solutions were mixed with water (in a 60 : 40 ratio) to improve the chromatographic peak shapes. An aliquot of 5 μL of this solution was injected (with a SIL-20A autosampler) into a HPLC system consisting of a Shimadzu LC-20AD XR pump, and a SCL-10A VP system controller (Shimadzu, Kyoto, Japan). The LC system was run in the isocratic mode with a flow of 0.2 mL min^{-1} and a mobile phase consisting of varying mixtures of methanol and sub-boiled water (40, 45, 50, 55, 60, 70 and 80%) containing 0.2 mM ammonium acetate in order to favour ionization conditions in the ESI-MS system.[35] Measuring time depended on ϕ_{MeOH} and chain length of the PFAAs, and varied from 5 min to 60 min. Analytes were detected with a tandem mass spectrometer (4000 Q Trap; Applied Biosystems, Toronto, Canada) operating in the negative ionization mode. Mass transitions applied for all analytes measured are shown in Table SI.1 in the ESI.†

2.4 Calculations

The partition coefficients between PFAAs and the sorbent materials were determined using a chromatographic retention method similar to that described previously.[4] Briefly, the retention time or first moment (t_R, in min) of an analyte injected on a column with a sorbent material, was corrected for the dead volume t_0 (see Table SI.2†) and multiplied with the flow rate (Q, in mL min^{-1}) to yield the retention volume for one measurement (V_R in mL). This volume, divided by the total mass (m in g) of the column sorbent gives the partition coefficient (K_D in mL g^{-1} adsorbent) for a specific eluent composition (eqn (1)).

$$K_D = \frac{(t_R - t_0)Q}{m_{sorbent}} \qquad (1)$$

Because no elution occurred if the analytes were injected in a mobile phase consisting of pure water, such as observed in the previous study,[4] methanol was used as organic modifier. When the $\ln K_D$ values obtained with different organic modifier contents in the mobile phase were plotted against the volume fraction of methanol (φ), straight lines were obtained that could be extrapolated in order to estimate the $\ln(K_{D,0})$ with 100% water:

$$\ln(K_D) = \phi \cdot S_n + \ln(K_{D,0}) \qquad (2)$$

with a slope S_n that depends on the length of the CF_2 chain. The 95% prediction interval of extrapolation to $K_{D,0}$ was calculated from the regression line and is reflected in the error bars (see the Results section).

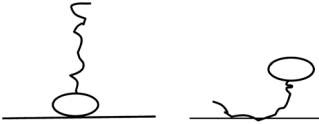### 2.5 Sorption model of surfactants

PFAAs as an example of a specific type of surfactants can adsorb both by their head (electrostatic interaction) and/or tail (hydrophobic interaction) to an adsorbent and the main issue is how to model the overall interaction of PFAAs with at least two different adsorbents. Currently two models have been described in the literature, the Virial and NICA-Dannon one.[28]

In both these models the overall standard Gibbs energy of adsorption of a molecular PFAA moiety, $\Delta_s G_{total}^{0,molec}$ (kJ mol^{-1}) is the sum of its hydrophobic and electrostatic contribution at its specific sorption location. This molecular DM model is depicted in Table 2. It is assumed that at environmentally relevant concentrations no other molecular surfactant interactions (e.g. between surfactant moieties themselves) are present. Consequently the total molecular sorption constant, K (L mmol^{-1}), is a product of the electrostatic, K^{elec}, and hydrophobic interaction energies, K^{hydr}, being $K^{elec} \times K^{hydr}$ since $K^{total} = \exp(-\Delta_s G_{total}^{0,molec}/RT)$. If each sorption location can only be filled with one PFAA moiety and all PFAA moieties are attached to these locations by the same sorption energy then the Langmuir conditions are fulfilled and K refers to the Langmuir sorption constant, K_L. In that case the DM model of the combined interaction with two adsorbents leads to one Langmuir sorption isotherm where K_L^{total} is given by the product of the electrostatic and hydrophobic interaction and a specific value of $C_{s,max}^{hydr+elec}$ (mmol kg^{-1} sediment) representing the total number of possible sorption locations on the combined adsorbents where the PFAA moiety can interact both by the head (electrostatic) and tail (hydrophobic) simultaneously (see Table 2).

In the recently developed IM model[32] it is assumed that in sediment or soil sorption experiments the hydrophobic moiety (tail) of the PFAA can adsorb to one adsorbent location while the electrostatic moiety (head) of the PFAA can adsorbed to another adsorbent location. Therefore only one part of the PFAA moiety is involved in an adsorption process, either the head or the tail. The molecular picture of this model is also depicted in Table 2. The overall standard Gibbs energy of sorption for the IM model is not simply the sum of both interaction terms anymore but the overall sorption constant, K^{total} is now the sum of the different sorption constants, $K^{elec} + K^{hydr}$. This leads to a different expression of $\Delta_s G_{total}^{0,molec}$ (see Table 2). If each sorption location can only be filled with one PFAA moiety and all PFAA moieties are attached to these locations by the same sorption energy then the Langmuir conditions are fulfilled and K refers to the Langmuir sorption constant, K_L. Therefore the IM model of the combined interaction leads to an overall adsorption isotherm consisting of two Langmuir sorption isotherms, one for the hydrophobic interaction by the tail (K_L^{hydr}) and other one for the electrostatic interaction by the head (K_L^{elec}), each having their own number of sorption locations $C_{s,max}^{hydr}$ and $C_{s,max}^{hydr}$ (mmol kg^{-1} sediment) (see Table 2). The Freundlich isotherm is not appropriate because the sorption model is ill defined and the isotherm is merely empirical.

When comparing scientific literature on sorption experiments of surfactants it turned out that the results could only be interpreted correctly with the IM model.[32] This is caused by the

This journal is © The Royal Society of Chemistry 2021

Environ. Sci.: Processes Impacts, 2021, **23**, 1997–2006 | **1999**

Table 2 Relevant mathematical adsorption expressions of the DM and IM model

	Dual-Mode (DM)	Independent Mode (IM)
Molecular sorption model		
Total standard Gibbs energy of the molecular sorption process ($\Delta_s G_{\text{total}}^{0,\text{molec}}$)	$\Delta_s G_{\text{total}}^{0,\text{molec}} = \Delta_s G_{\text{elec}}^{0,\text{molec}} + \Delta_s G_{\text{hydr}}^{0,\text{molec}}$	$\Delta_s G_{\text{total}}^{0,\text{molec}} = -RT\ln\{\exp(-\Delta_s G_{\text{elec}}^{0,\text{molec}}/RT) + \exp(-\Delta_s G_{\text{hydr}}^{0,\text{molec}}/RT)\}$
Total Langmuir sorption isotherm in the molecular description	$C_s = \dfrac{(K_{\text{L,elec}}^{\text{molec}} \times K_{\text{L,hydr}}^{\text{molec}}) \times C_{\text{s,elec+hydr}}^{\max} \times C_w}{1 + K_{\text{L,elec}}^{\text{molec}} \times K_{\text{L,hydr}}^{\text{molec}} C_w}$	$C_s = \dfrac{K_{\text{L,elec}}^{\text{molec}} \times C_{\text{s,elec}}^{\max} \times C_w}{1 + K_{\text{L,elec}}^{\text{molec}} C_w} + \dfrac{K_{\text{L,hydr}}^{\text{molec}} \times C_{\text{s,hydr}}^{\max} \times C_w}{1 + K_{\text{L,hydr}}^{\text{molec}} C_w}$
Sorption isotherm at infinite dilution in the molecular and in the partition description	$C_s = (K_{\text{L,elec}}^{\text{molec}} \times K_{\text{L,hydr}}^{\text{molec}}) \times C_{\text{s,elec+hydr}}^{\max} \times C_w,$ $C_s = (K_{\text{p,0}}^{\text{elec}} \times K_{\text{p,0}}^{\text{hydr}}) \times C_w$	$C_s = K_{\text{L,elec}}^{\text{molec}} \times C_{\text{s,elec}}^{\max} \times C_w + K_{\text{L,hydr}}^{\text{molec}} \times C_{\text{s,hydr}}^{\max} \times C_w$ or $C_s = (K_{\text{L,elec}}^{\text{molec}} \times C_{\text{s,elec}}^{\max} + K_{\text{L,hydr}}^{\text{molec}} \times C_{\text{s,hydr}}^{\max}) \times C_w,$ $C_s = (K_{\text{p,0}}^{\text{elec}} + K_{\text{p,0}}^{\text{hydr}}) \times C_w$

fact that the mathematical expression of the total standard Gibbs energy of the molecular sorption process of the DM model can be derived from the IM model if one of the two interaction energies is much larger than the other one since if $\delta \ll 1$, $\ln(1 + \delta) \approx \delta$. The Virial or NICA-Donnan model does not work when this condition is not fulfilled leading to difficulties in applying these models in other experiments. Although the mathematical expression of the DM can be derived from the IM its physical picture of sorption processes of the IM model has not changed when one of the interaction energies is much larger. In addition it is also quite difficult to understand how a sorption location will look like if both adsorbents are present and how these locations must have been formed if these two adsorbents are mixed. Therefore at low or environmentally relevant concentrations the IM model best describes to date the adsorption isotherm when both the head and the tail of a surfactant is involved in an adsorption process.

In a simple PFAA sorption experiment a certain amount of adsorbent with a final number of sorption locations is combined with a dissolved amount of PFAA. At equilibrium the PFAA fraction adsorbed depends then on the number of sorption sites occupied in the experimental system and the corresponding K-value. This leads to a ratio of adsorbed PFAA to the adsorbent, C_s, in equilibrium with the dissolved fraction of PFAA. C_w, denoted as the partition coefficient K_p (L kg^{-1}). Thus K_p and K are two different equilibrium constants referring to two different thermodynamic systems, the experimental one and the molecular one respectively, but are related to each other. This relationship is governed by the applied sorption model where at low and environmentally relevant concentrations the Langmuir is applied most often.

The relationship between K_p and K_L can be seen when conducting a sorption experiment. At the start of the sorption experiment the fraction of the PFAA adsorbed to the sediment will be proportional to the concentration of the PFAA and therefore the partition constant, K_p, does not vary with the PFAA concentration (Henry's law region), $K_{p,0}$ (L kg^{-1} sediment). This region is called the infinite dilution region and the corresponding Langmuir sorption isotherm in the molecular and

partition description is also included in Table 2. In this case the $K_{p,0}$ is related to K_L by eqn (3) [32,33]

$$K_{p,0} = K_L \times C_s^{\max} \qquad (3)$$

As soon as the number of sorption locations becomes saturated, less and less PFAA will be sorbed to the remaining empty locations and the partition constant, K_p, will start to decrease until it has reached a value of zero (0) when all sorption locations have been occupied but the value of K_L itself is not affected. Consequently the partition constant is a function of the concentration of the PFAA, $K_p(C_w)$.[32] This implies that when for modelling purposes the value of K_L is required, one must first confirm that the measured partition constant is in the Henry's law region. In that case the K_L value can only be found if $C_s^{\max}$, is also known which can only be determined if the complete Langmuir isotherm is established.

It is clear that for sorption remediation technologies K_p, will be the relevant parameter but for modelling it is K_L. Therefore if one would like to know which adsorbent is more effective to remove PFAA, their $K_{p,0}$ values must be compared to each other. In case a difference in $K_{p,0}$ is found for the same PFAA, it is still not known if this difference is caused by a difference in sorption constant of the PFAA, K_L or a difference in $C_{s,\max}$ (or both) *cf.* eqn (3). For example, varying the pH may lead to a varying $K_{p,0}$, but only if at both pH-values the complete Langmuir has been established one may conclude which of the two parameters (or both) may have changed.

Finally in case only an electrostatic or hydrophobic adsorption process occurs for PFAAs with varying CF$_2$ groups, N_{CF_2}, the standard Gibbs energy of the sorption process of the next PFAA, $\Delta_s G^0(N + 1)_{\text{CF}_2}$ can be obtained by assuming that the incremental standard Gibbs energy for each N_{CF_2}, $\Delta\Delta_L G^0$, is constant.

From eqn (3) it can then be deduced[32] that $\Delta_s G^0(N_{\text{CF}_2})$ for an electrostatic adsorption process only, with varying CF$_2$ groups (N_{CF_2}) can be represented by eqn (4a):

$$\Delta_s G_{\text{elec}}^0(N_{\text{CF}_2}) = \Delta_L G_{\text{head-surf}}^0 + \Delta\Delta_L G_{\text{tail-water}}^0 \times N_{\text{CF}_2} - RT\ln C_{\text{s,anionic}}^{\max} \qquad (4a)$$

2000 | *Environ. Sci.: Processes Impacts*, 2021, **23**, 1997–2006

This journal is © The Royal Society of Chemistry 2021

And similarly, for an hydrophobic adsorption process only:

$$\Delta_s G^0_{hydr}(N_{CF_2}) = \Delta_L G^0_{tail-surf} + \Delta\Delta_L G^0_{head-water} \\ \times N_{CF_2} - RT \ln C^{max}_{s,hydr} \qquad (4b)$$

Assuming that $\Delta\Delta_L G^0$ is constant but only varies for the different types of interaction, a plot of $\Delta_s G^0_{elecorhydr} = -RT\ln(K_{p,0})$ vs. N_{CF_2} will give a straight line with a slope that varies only for the type of interaction. Thus a constant slope for different unbranched PFAA adsorbents supports the interpretation that only a single specific type of interaction is present in this sorption process. However the intercept of this plot $\Delta_s G^0(0)$, includes not only the standard Gibbs energy contribution of surface adsorption term, $\Delta_L G^0_{surfaceterm}$, but also the contribution of the total number of sorption sites $-RT\ln C^{max}_s$.

3. Results

3.1 Validation

The standard deviation of the retention time for multiple injections of one standard solution (PFOA) was low, e.g., in a series of repeated experiments with the C_{18} column the average t_R was 5.849 and the standard deviation was $\pm$ 0.088 min. In our experiments a minimum of four standard solutions with different concentrations were analysed in duplicate. Examples of peak shapes of PFPA from 30% to 100% MeOH are shown in the ESI (Fig. SI.3.1†). The concentrations injected were all within the linear dynamic range of the LC-MS/MS system used and lead to C_w values in the order of μg L^{-1} which are far below the critical micelle concentrations (CMC) of the selected PFAAs (data not shown). CMCs for PFAAs range from around 156 000 to 14 mg L^{-1} for N_{CF_2} from 4–14.[36] Within the applied experimental range no influence of the concentration on the retention time (and thus on the K_D) was observed, only the response (area) of the peak increased. This shows that the partition coefficient is independent of the PFAA concentration and the experiments are conducted in the infinite dilution range, where $K_{p,0}$ applies according to the previously introduced IM model and thus the derived $K_D = K_{p,0}$. In total a minimum of eight results per PFAA mobile phase composition and sorbent material were used in order to calculate an average value of the t_R and $K_{p,0}$. Since PFAAs are deprotonated at environmentally relevant pH (about 7), the pH was not a variable during the experiments.

The $\ln K_{p,0}$ values obtained with different fractions of methanol in the mobile phase were extrapolated back to 100% water using a linear fit and the 95% confidence interval was calculated. The values of R^2 of the regressions lines of each PFAA on each adsorbent are shown in Table SI.3.2.† Linearity up to 100% water of PFBA on a C18 column has been shown before[4] and the reasons that linearity of longer chain PFAAs in the range of 40% to 80% methanol is present, were discussed in the same reference. In the same reference it has been shown that the pH has no significant effect on the log k' values, which indicates the absence of an electrostatic interaction between C_{18} and the PFAAs in the investigated pH range and that therefore only hydrophobic interaction occurs. Given the even slightly better
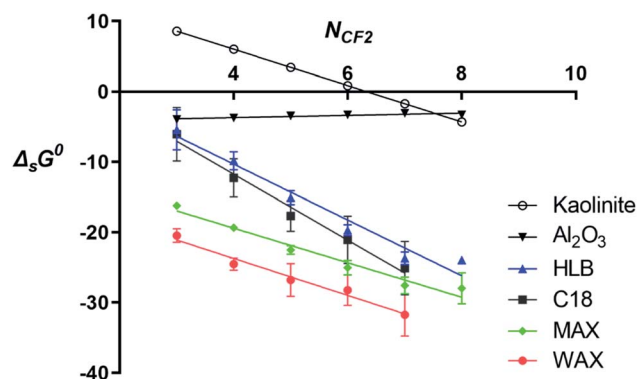

Fig. 1 Plot of N_{CF_2} of the sorbates vs. $\Delta_s G^0$ (in kJ mol^{-1}) for our five different adsorbents. The error bars represent the 95% confidence interval from the extrapolation to 100% water. The kaolinite values are taken from literature from Xiao et al. (2011).

values of R^2 for the similar experiments when using a WAX or MAX column supports the linearity of the capacity factor with the methanol fraction when similar PFAA experiments are conducted with the positively charged columns WAX and MAX. All $\ln(K_{p,0})$ vs. %MeOH plots are shown in Fig. SI.3.2–3.2.6.† The $\ln K_{p,0}$ values are converted into ΔG^0_s by multiplying with $-RT$ where R is the gas constant and T is the room temperature taken as 300 K and shown in Table SI.3.3.†

3.2 Standard Gibbs energy of adsorption to sorbents, $\Delta_s G^0$

Experimentally derived $\Delta_s G^0$ stated in Table SI.3† are plotted vs. N_{CF_2} for different adsorbents. The resulting graphs are shown in Fig. 1.

The corresponding values for the slope and the intercept are presented in Table 3. It is assumed in this paper that these values are also valid for PFAAs above or below the tested range ($N_{CF_2} < 3$ or $N_{CF_2} > 8$). The adsorbents tested are discussed below in order of increasing polarity and the incremental standard Gibbs energy of adsorption, $\Delta\Delta_L G^0$, is discussed in Section 3.3.

For C_{18} the standard Gibbs energy of sorption, $\Delta_s G^0_{C18}$, shown in Fig. 1 becomes more favourable with increasing number of N_{CF_2} units within the PFAA homologue series studied. In our experimental set-up it is expected that only PFAAs with $N_{CF_2} \geq 3$ will lead to $\Delta_s G^0_{C18} < 0$ and therefore show substantial adsorption. Hence, longer chain PFAAs, such as PFOA ($\Delta_s G^0_{C18}(7) = -25.9 \pm 3.8$ kJ mol^{-1}) are shown to adsorb better than shorter chain PFAAs such as PFBA ($\Delta_s G^0_{C18}(3) = -6.1 \pm 3.8$ kJ mol^{-1}). The interactions of the C_{18} material and the PFAA molecule are expected to have only hydrophobic character (van der Waals interactions) and to occur between the tail of the PFAA, and the alkyl chains of the C_{18} material (see Fig. SI.4.1†). No electrostatic interactions of the head with the C_{18} material are observed by a variation in retention time, peak broadening or additional peaks seen. In addition the AEC of C_{18} material is non-existent (see Table 1) and the value of the intercept in Fig. 1 is positive ($+7.0 \pm 1.7$ kJ mol^{-1}).

HLB is a neutral polymer with aromatic and amide groups (see Fig. SI.4.2†). The adsorption results show that the $\Delta_s G^0_{HLB}$ of

This journal is © The Royal Society of Chemistry 2021

Environ. Sci.: Processes Impacts, 2021, **23**, 1997–2006 | **2001**

PFBA to PFOA are slightly higher than that of C_{18} and therefore its $K_{p,0}^{HLB}$ is slightly lower. However this difference is not statistically significant. As is the case for C_{18}, it is expected that only PFAAs with $N_{CF_2} \geq 3$ will lead to $\Delta_s G_{HLB}^0 < 0$ and therefore to a substantial adsorption onto HLB.

The WAX polymer has two different types of adsorption sites (see Fig SI.4.3†). The first consists of the positively charged N atoms ($pK_a \approx 6$) which can have electrostatic interactions with the negatively charged head groups of PFAAs (AEC = 7.23×10^{-7} mol m^{-2}). Secondly, the apolar matrix of the WAX (which is similar to HLB) can interact with the hydrophobic tail of the PFAA, and these interactions would refer to a hydrophobic sorption mechanism. Our experimental results show that the intercept of WAX equals -13 ± 1.3 kJ mol^{-1}) which is much more favourable than that of C_{18} ($+7.0 \pm 1.7$ kJ mol^{-1}) (see Table 3). The extra electrostatic interaction of the head of the PFAA to the N-atom in the adsorbent is the main cause of this large energy difference.

The slope of the plot is similar to that of kaolinite[37] and MAX indicating that only the electrostatic interaction is involved. Any possible hydrophobic adsorption to the HLB-like matrix therefore does not seem to occur at our applied experimental conditions.

MAX is a polymer similar to WAX with two different types of adsorption sites, the first consisting of permanently charged N atoms, which in contrast to WAX are not permanently charged, and the second an apolar matrix similar to HLB (see Fig SI.4.3†). The mean value of the intercept for this sorbent amounts to -9.6 ± 1.3 kJ mol^{-1} (see Table 3), caused by the electrostatic interactions with the positively charged N atoms. Although the charge on the nitrogen is permanent the intercept of MAX is higher and its $K_{p,0}$ is lower than that observed for the WAX sorbent (-9.6 vs. -13 kJ mol^{-1}). However according to eqn (3) when a variation in the measured partition coefficients between MAX and WAX for the same PFAA is observed this variation may be caused by either a variation in K_L corresponding to a stronger interaction of the PFAA to the adsorbent or a variation in the sorption capacity, $C_{S,elec}^{max}$, because more sorption sites per kg adsorbent are present. In order to distinguish between these two factors a comparison of AEC values (see Table 1) between both adsorbents, WAX and MAX, assuming that their AEC-values correlate to $C_{S,elec}^{max}$. The AEC of WAX is around 2.4 times larger than that of MAX. This suggests that the number of available sorption sites and thus $C_{S,elec}^{max}$ for WAX is 2.4 times larger than that for MAX. This will lower the value of $\Delta_s G_{MAX}^0$ with $-RT\ln 2.4 = -2.2$ kJ mol^{-1}, thereby explaining a large part of the difference of -3.4 kJ mol^{-1} between the values of $\Delta_s G^0$ for WAX and MAX. Therefore it seems that the variation in $K_{p,0}$ between MAX and WAX for PFAA is mainly caused by the difference in sorption capacity, $C_{S,elec}^{max}$, rather than a difference in sorption affinity (K_L) of the PFAA with the adsorbent.

Despite the slightly weaker adsorption affinity of MAX than of WAX, the interactions of the head combined with the possibly moderate interaction of the tail makes both ion exchange polymers very suitable as sorbents for both short and long chain PFAAs.

Al_2O_3 Interestingly, Al_2O_3 shows only little adsorption and a slight positive slope for each N_{CF_2}. Table 3 indicates that the AEC-value Al_2O_3 is 0.10 mmol kg^{-1} (see Table 1) which is substantially lower than for WAX or MAX. Therefore one factor of this reduced adsorption capacity may be caused by the limited number of suitable sorption locations on Al_2O_3 for PFAA in the applied experimental conditions.

3.3 Differential standard Gibbs energy of adsorption, $\Delta\Delta_L G^0$

Table 3 shows that the slopes ($\Delta\Delta_L G^0$) of the hydrophobic materials C_{18} (-4.7 ± 0.34 kJ mol^{-1}) and HLB (-4.0 ± 0.40 kJ mol^{-1}), are not significantly different from each other. As a comparison, standard Gibbs energy of transfer of different PFAAs from octanol into water ($\Delta_{OW} G^0$) was calculated using the SPARC model-predicted K_{ow} data from Arp and co-workers.[38] The $\Delta_s G_{C18}^0(5, 6, 7)$ for PFHxA, PFHpA and PFOA of -18; -21 and -25 kJ mol^{-1} calculated in the present study correspond almost exactly to $\Delta_{OW} G^0$ values of -17; -21; -25 kJ mol^{-1} for PFHxA, PFHpA and PFOA, respectively. The similarity of the structures of octanol and C_{18} material and consequently similar type of interaction with PFAAs is a likely explanation for this agreement. As our sorption experiments show, the hydrophobic contribution of the tail depends on the type of interaction. Therefore one needs to be careful to compare the differential contribution of a CF_2-group in our sorption experiments with contributions derived from other hydrophobic parameters like the K_{ow}. Comparing for example our values with experimentally derived K_{ow} values by applying an external electrostatic potential to a water and octanol interface as is done in cyclic voltammetry is not advisable since in such an experiment the K_{ow}-value likely includes the hydrophobic effect of the electrostatic interaction.[39] The SPARC model is more appropriate since in this model only the contribution of the octanol itself is incorporated.

This finding shows that when only hydrophobic interactions are expected in the adsorption process of PFAAs the slope is independent of the type of adsorbent applied and around a value of ≈ -4.4 kJ mol^{-1}. The HLB polymer structure also contains amide groups that may be available for sorption. However, given the similarity of the $\Delta\Delta_L G^0$ values of HLB and C_{18}, we can conclude here that under the applied experimentally conditions no substantial interaction with the amide group seem to occur in our experimental setup.

Table 3 Mean values of the intercepts ($\Delta_s G^0(0)$) and slopes ($\Delta\Delta_L G^0$) of the ln K_D vs. N_{CF_2} relationships for each sorbent

Sorbent	$\Delta_s G^0(0) \pm 95\%$ CI (kJ mol^{-1})	$\Delta\Delta_L G^0 \pm 95\%$ CI (kJ mol^{-1})
C_{18}	+7.0 ± 1.7	−4.7 ± 0.34
HLB	+5.5 ± 2.3	−4.0 ± 0.40
WAX	−13 ± 1.3	−2.6 ± 0.24
MAX	−9.6 ± 1.3	−2.5 ± 0.23
Al_2O_3	−4.3 ± 0.22	0.16 ± 0.04
Octanol		−4.7[a]
Kaolinite	+16	−2.6[b]
Org matter		−3.4[c]

[a] Calculated (with the SPARC data) from Arp et al. (2006).[38] [b] Calculated from Xiao et al. (2011).[37] [c] From Higgins and Luthy (2007).[30]

2002 | Environ. Sci.: Processes Impacts, 2021, **23**, 1997–2006

This journal is © The Royal Society of Chemistry 2021

The $\Delta\Delta_L G^0$ values of the interaction between PFAAs and WAX, MAX and kaolinite are also not significantly different from each other (~-2.6 kJ mol^{-1}) but do differ significantly from those for HLB, C_{18} and octanol. Data for sorption of PFAAs onto kaolinite, a zeolite clay were taken from Xiao *et al.*,[37] using the lowest Na$^+$ concentration (log[Na$^+$] = 10$^{-3.00}$ mol L^{-1}). It is expected that only an electrostatic sorption process of the head prevails for this adsorbent. The electrostatic repulsion of the negatively-charged PFAA head and the negatively charged kaolinite leads then to a $\Delta_s G^0(0) \gg 0$ which is observed. In the experimental set-up with kaolinite [Na$^+$] remains constant and only for $N_{CF_2} > 7$ does $\Delta_s G^0_{kaolinite}$ become negative, indicating that substantial sorption will only occur for longer chain PFAAs.

Finally, the value of $\Delta\Delta_L G^0$ for sorption to organic matter[30] (-3.4 kJ mol^{-1}, Table 3) is exactly intermediate between the values of $\Delta\Delta_L G^0$ for the hydrophobic and the electrostatic interactions of PFAA (($-4.4 + -2.6$)/2). This agrees with an independent mode if both adsorption processes are present.[32] In addition establishing the value of the slope with a specific adsorbent under the condition that the linear sorption isotherm is valid can distinguish clearly if only a hydrophobic or an electrostatic interaction is present or that both interactions occur at the same time in the applied experimental system. The value of the slope is also expected to be independent of the ionic strength of the solution.[37]

4. Discussion

In this section we discuss the sorption parameters that are most relevant to select the optimal adsorbents to remove both the short chain and long chain PFAAs from contaminated waters. From our measurements it can be deduced that adsorbents with a positively charged functional group (such as WAX and MAX) have a higher sorption affinity for the short chain PFAAs than hydrophobic materials (such as C_{18} and HLB). For example, one can compare the adsorption affinity in terms of removal of PFBA ($N_{CF_2} = 3$) by WAX ($\Delta_s G^0_{WAX} = -20.5$ kJ mol^{-1}) and HLB ($\Delta_s G^0_{HLB} = -5.4$ kJ mol^{-1}) at room temperature *cf.* eqn (5):

$$\frac{K_{p,0}^{WAX}}{K_{p,0}^{HLB}} = \exp\left[\frac{-(-20.5 - (-5.4))}{RT}\right] \approx 450 \qquad (5)$$

After eqn (4a) and (4b) and using the ΔG-values from Table 3 for WAX and HLB, respectively, one can deduce that only beyond $N_{CF_2} = 13$, (PFTeDA) does the $K_{p,0}$ of HLB becomes higher than that of WAX (see also Fig. 2). As stated in Section 2.5 based on the individually derived $K_{p,0}$ values of HLB and WAX in our experiment (see Table SI.6.1†) one can estimate the overall partition coefficients, $K_{p,0}^{total}$, according to the IM and DM model when both adsorbents are mixed together. Both the individual and combined infinite dilution partition coefficients, calculated according to the IM and DM model, of PFAAs with N_{CF_2} varying from 1 to 14 are shown in Fig. 2.

It has been observed in PFAA sorption experiments on different soils that the chain-length *vs.* partition coefficient relationship decreases from longer chain PFAAs to shorter chain PFAAs but increases again for the smaller PFAAs notably PFBA and PFPeA.[40] This is a logical consequence of the IM model but not of the DM model. The DM model leads only to one Langmuir isotherm to express the sorption process of the combined effect. Since the $K_{p,0}^{total}$-values of the DM model only decreases proportionally, a single Langmuir sorption isotherm will lead to less and less PFAA sorption by shorter chain PFAA. This is different for the IM model. For long chain PFAAs the hydrophobic partition coefficient, $K_{p,0}^{hydr}$, is dominant over the electrostatic one, $K_{p,0}^{elec}$ ($K_{p,0}^{hydr} \gg K_{p,0}^{elec}$). When extrapolating to short chain PFAAs only an extrapolation of the hydrophobic contribution is applied and therefore the hydrophobic contribution will decrease proportionally. However for short chain PFAAs the electrostatic contribution will take over because at shorter chain PFAA $K_{p,0}^{elec}$ becomes higher that $K_{p,0}^{hydr}$. Therefore an extra sorption term will appear for shorter chain PFAAs leading to an increase of sorption for shorter chain PFAAs, as is observed.

The IM sorption model will show a varying fraction of PFAA adsorbed on either the HLB or WAX adsorbent in a batch experiment when both adsorbents are mixed together. Such a picture cannot be made with the DM model since it is unknown how both adsorbents will have combined to create their DM sorption locations. The different fractions adsorbed for each PFAA on either WAX or HLB according to the IM model can also be predicted, (see SI.V† for the relevant methodology). If a sorption experiment is conducted in 1 L of water where for
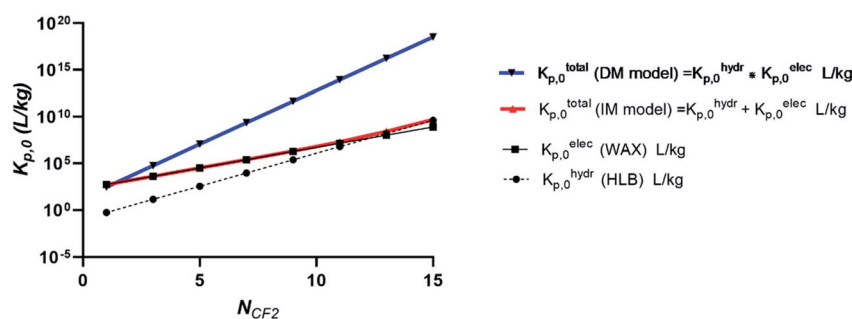

Fig. 2 Infinite dilution partition coefficients of PFAAs for WAX and HLB independently (black) and for a system with a mixture of WAX and HLB according to the IM (red) and DM (blue) model. $K_{p,0}$-values with $N_{CF_2} > 8$ or $N_{CF_2} < 3$ are estimated by assuming that the linearity for each adsorbent as shown in Fig. 1 still holds.
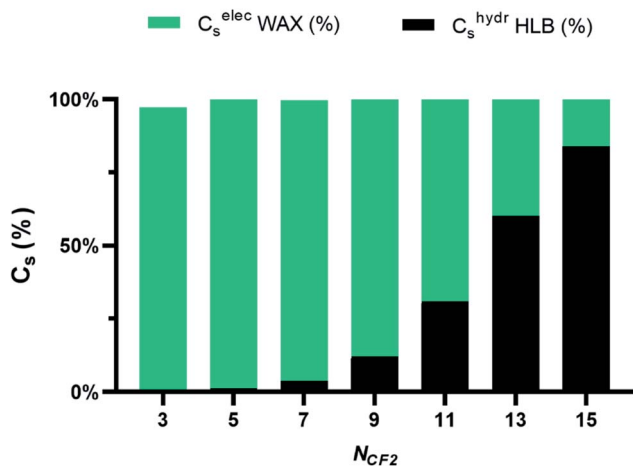
Fig. 3 Estimated fraction of a specific PFAA adsorbed by WAX (green) and HLB (black) conducted in a batch experiment in 1 L of water with 10 g of both adsorbents and a PFAA starting mass of 100 nmol. C_s (%) values above $N_{CF_2} > 8$ are estimated by assuming that the linearity for each adsorbent as shown in Fig. 1 still holds.

example 100 nmol of a specific PFAA and 10 grams of HLB and WAX adsorbent with the characteristics from Table 1 have been added together and adsorption occurs in the Henry's law region the adsorption efficiency of the HLB/WAX mixture is expected to vary from 97.66% for PFC$_4$A to 99.9999980% for PFC$_{14}$A (see Table SI.6.2†) but the adsorbed fractions on either WAX or HLB vary strongly as can be seen in Fig. 3.

Since PFAAs contain both a hydrophobic moiety and an electrostatic moiety the best selection of adsorbents for remediation technologies according to the IM model are ones with high K_L^{elec} and high $C_{S,elec}^{max}$ for the electrostatic adsorbent like WAX, and high K_L^{hydr} and high $C_{S,hydr}^{max}$ for the hydrophobic adsorbent like HLB. In addition the electrostatic adsorbent which is important to remove the shorter chain PFAAs is most effective if its sorption locations can no longer be occupied by the longer chain PFAAs since even for this electrostatic interaction $K_{p,0}^{elec}$ increases with increasing N_{CF_2}. These long chain PFAAs with their often dominant hydrophobic interaction can be removed first by a hydrophobic adsorbent e.g. HLB. This will leave the short chain PFAAs still in solution but these ones can now be removed more efficiently by an electrostatic adsorbent e.g. WAX. All the sorption locations present at the electrostatic adsorbent are then only used to adsorb the short chain PFAAs. Thus according to the IM model a two step sorption remediation technology, starting with a hydrophobic adsorbent followed by an electrostatic one, both with as high as possible C_s^{max}, is the most efficient adsorption remediation technology for PFAAs contaminated waters rather than mixing these types of adsorbents. Based on our results the Al$_2$O$_3$ adsorbent is less appropriate for removing PFAAs from relevant water systems.

In PFAA sorption experiments conducted with soil or sediment it is not clear which specific adsorbents are involved and how to estimate the $K_{p,0}$-values required in risk assessments. In this case the K_L^{hydr} and $C_{S,hydr}^{max}$, and the K_L^{elec} and $C_{S,elec}^{max}$ must be estimated from the soil/sediment sample. While for the

K_L^{hydr} many estimation methods exists in the form of K_{oc} estimation methods, this does not count for K_L^{elec}. In addition corresponding $C_{S,hydr}^{max}$ and $C_{S,elec}^{max}$ values must also be estimated. In this respect the most important soil/sediment parameters that seem to be related to these C_s^{max} values are soil organic carbon fraction (f_{oc}) for $C_{S,hydr}^{max}$ which is well established, and the AEC for $C_{S,elec}^{max}$ in case of anionic surfactants like PFAAs.[41] However, firstly the exact relationship between f_{oc} and $C_{S,hydr}^{max}$ and therefore also between K_{oc} and K_L^{hydr} is not well established and secondly it is still early to conclude that AEC is indeed a suitable descriptor for $C_{S,elec}^{max}$. It also shows clearly why for example a correlation between electrostatic surfactants with a negatively charged head, e.g., PFAAs and the CEC is hardly found since the CEC is strongly correlated to adsorption by a positively charged surfactant.

If, as assumed in the present study, the AEC is a suitable descriptor for $C_{S,elec}^{max}$ of an anionic surfactant and its value is expressed in µmol m^{-2} as is often done (see Table 1), then $C_{S,elec}^{max}$ expressed in µmol kg^{-1} as in eqn (3) is also a function of the surface area and the $K_{p,0}$ will increase when the surface area increases or the particle diameter decreases e.g. comparing fine and course soil size fractions.[17,42] This increase in $K_{p,0}$ with decreasing particle size is therefore not caused by an increasing adsorption strength of the surfactant moiety to the adsorbent, K_L. but by an increase of $C_{S,elec}^{max}$ in the applied experimental system and therefore the smaller the grains for the specific adsorbent the higher its $C_{S,elec}^{max}$ (mmol kg^{-1} sediment) leading to a higher $K_{p,0}$-value cf. eqn (3), the better the adsorption remediation technology will work as expected.

Conflicts of interest

There are no conflicts to declare.

Acknowledgements

References

1 R. C. Buck, J. Franklin, U. Berger, J. M. Conder, I. T. Cousins, P. de Voogt, A. A. Jensen, K. Kannan, S. A. Mabury and S. P. J. van Leeuwen, Perfluoroalkyl and polyfluoroalkyl substances in the environment: Terminology, classification, and origins, Integr. Environ. Assess. Manage., 2011, 7, 513–541.

2 K. Goss, The p K a values of PFOA and other highly fluorinated carboxylic acids, Environ. Sci. Technol., 2008, 42, 456–458.

3 L. Vierke, U. Berger and I. T. Cousins, Estimation of the acid dissociation constant of perfluoroalkyl carboxylic acids

through an experimental investigation of their water-to-air transport, *Environ. Sci. Technol.*, 2013, **47**, 11032–11039.

4 P. de Voogt, L. Zurano, P. Serné and J. J. Haftka, Experimental hydrophobicity parameters of perfluorinated alkylated substances from reversed-phase high-performance liquid chromatography, *Environ. Chem.*, 2012, **9**, 564–570.

5 M. L. Brusseau, R. H. Anderson and B. Guo, PFAS concentrations in soils: Background levels *versus* contaminated sites, *Sci. Total Environ.*, 2020, **740**, 140017.

6 L. Ahrens, Polyfluoroalkyl compounds in the aquatic environment: a review of their occurrence and fate, *J. Environ. Monit.*, 2011, **13**, 20–31.

7 European Commission, 2021, https://ec.europa.eu/ environment/pdf/chemicals/2020/10/SWD_PFAS.pdf.

8 R. Vestergren and I. T. Cousins, Tracking the pathways of human exposure to perfluorocarboxylates, *Environ. Sci. Technol.*, 2009, **43**, 5565–5575.

9 C. Eschauzier, J. Haftka, P. Stuyfzand and P. de Voogt, Perfluorinated compounds in infiltrated river rhine water and infiltrated rainwater in coastal dunes, *Environ. Sci. Technol.*, 2010, **44**, 7450–7455.

10 C. Eschauzier, M. Hoppe, M. Schlummer and P. de Voogt, Presence and sources of anthropogenic perfluoroalkyl acids in high-consumption tap-water based beverages, *Chemosphere*, 2013, **90**, 36–41.

11 H. N. P. Vo, H. H. Ngo, W. Guo, T. M. H. Nguyen, J. Li, H. Liang, L. Deng, Z. Chen and T. A. H. Nguyen, Poly-and perfluoroalkyl substances in water and wastewater: A comprehensive review from sources to remediation, *Journal of Water Process Engineering*, 2020, **36**, 101393.

12 D. M. Wanninayake, Comparison of currently available PFAS remediation technologies in water: A review, *J. Environ. Manage.*, 2021, **283**, 111977.

13 J. N. Meegoda, J. A. Kewalramani, B. Li and R. W. Marsh, A review of the applications, environmental release, and remediation technologies of per-and polyfluoroalkyl substances, *Int. J. Environ. Res. Public Health*, 2020, **17**, 8117.

14 C. Eschauzier, E. Beerendonk, P. Scholte-Veenendaal and P. De Voogt, Impact of treatment processes on the removal of perfluoroalkyl acids from the drinking water production chain, *Environ. Sci. Technol.*, 2012, **46**, 1708–1715.

15 V. A. A. Espana, M. Mallavarapu and R. Naidu, Treatment technologies for aqueous perfluorooctanesulfonate (PFOS) and perfluorooctanoate (PFOA): A critical review with an emphasis on field testing, *Environ. Technol. Innovation*, 2015, **4**, 168–181.

16 Y. Yao, K. Volchek, C. E. Brown, A. Robinson and T. Obal, Comparative study on adsorption of perfluorooctane sulfonate (PFOS) and perfluorooctanoate (PFOA) by different adsorbents in water, *Water Sci. Technol.*, 2014, **70**, 1983–1991.

17 C. Wu, M. J. Klemes, B. Trang, W. R. Dichtel and D. E. Helbling, Exploring the factors that influence the adsorption of anionic PFAS on conventional and emerging adsorbents in aquatic matrices, *Water Res.*, 2020, **182**, 115950.

18 R. Wang, C. Ching, W. R. Dichtel and D. E. Helbling, *Evaluating the Removal of Per-and Polyfluoroalkyl Substances from Contaminated Groundwater with Different Adsorbents Using a Suspect Screening Approach*, Environmental Science & Technology Letters, 2020.

19 C. Zeng, A. Atkinson, N. Sharma, H. Ashani, A. Hjelmstad, K. Venkatesh and P. Westerhoff, Removing per-and polyfluoroalkyl substances from groundwaters using activated carbon and ion exchange resin packed columns, *AWWA Water Sci.*, 2020, **2**, e1172.

20 N. Saeidi, F. Kopinke and A. Georgi, Understanding the effect of carbon surface chemistry on adsorption of perfluorinated alkyl substances, *Chem. Eng. J.*, 2020, **381**, 122689.

21 H. Son, T. Kim, H. Yoom, D. Zhao and B. An, The Adsorption Selectivity of Short and Long Per-and Polyfluoroalkyl Substances (PFASs) from Surface Water Using Powder-Activated Carbon, *Water*, 2020, **12**, 3287.

22 L. Zhao, J. Bian, Y. Zhang, L. Zhu and Z. Liu, Comparison of the sorption behaviors and mechanisms of perfluorosulfonates and perfluorocarboxylic acids on three kinds of clay minerals, *Chemosphere*, 2014, **114**, 51–58.

23 Z. Du, S. Deng, Y. Chen, B. Wang, J. Huang, Y. Wang and G. Yu, Removal of perfluorinated carboxylates from washing wastewater of perfluorooctanesulfonyl fluoride using activated carbons and resins, *J. Hazard. Mater.*, 2015, **286**, 136–143.

24 M. Sörengård, E. Östblom, S. Köhler and L. Ahrens, Adsorption behavior of per-and polyfluoralkyl substances (PFASs) to 44 inorganic and organic sorbents and use of dyes as proxies for PFAS sorption, *J. Environ. Chem. Eng.*, 2020, **8**, 103744.

25 H. N. Tran, S. You, A. Hosseini-Bandegharaei and H. Chao, Mistakes and inconsistencies regarding adsorption of contaminants from aqueous solutions: a critical review, *Water Res.*, 2017, **120**, 88–116.

26 D. P. Oliver, D. A. Navarro, J. Baldock, S. L. Simpson and R. S. Kookana, Sorption behaviour of per-and polyfluoroalkyl substances (PFASs) as affected by the properties of coastal estuarine sediments, *Sci. Total Environ.*, 2020, **720**, 137263.

27 F. Li, X. Fang, Z. Zhou, X. Liao, J. Zou, B. Yuan and W. Sun, Adsorption of perfluorinated acids onto soils: Kinetics, isotherms, and influences of soil properties, *Sci. Total Environ.*, 2019, **649**, 504–514.

28 M. W. Sima and P. R. Jaffé, A critical review of modeling Poly-and Perfluoroalkyl Substances (PFAS) in the soil-water environment, *Sci. Total Environ.*, 2020, 143793.

29 K. Y. Foo and B. H. Hameed, Insights into the modeling of adsorption isotherm systems, *Chem. Eng. J.*, 2010, **156**, 2–10.

30 C. P. Higgins and R. G. Luthy, Modeling sorption of anionic surfactants onto sediment materials: an *a priori* approach for perfluoroalkyl surfactants and linear alkylbenzene sulfonates, *Environ. Sci. Technol.*, 2007, **41**, 3254–3261.

31 F. Xiao, B. Jin, S. A. Golovko, M. Y. Golovko and B. Xing, Sorption and desorption mechanisms of cationic and zwitterionic per-and polyfluoroalkyl substances in natural

This journal is © The Royal Society of Chemistry 2021

Environ. Sci.: Processes Impacts, 2021, **23**, 1997–2006 | **2005**

soils: thermodynamics and hysteresis, *Environ. Sci. Technol.*, 2019, **53**, 11818–11827.

32 H. Krop, P. de Voogt, C. Eschauzier and S. Droge, Sorption of surfactants onto sediment at environmentally relevant concentrations: independent-mode as unifying concept, *Environ. Sci.: Processes Impacts*, 2020, **22**, 1266–1286.

33 P. S. Bäuerlein, T. L. Ter Laak, R. C. Hofman-Caris, P. de Voogt and S. T. Droge, Removal of charged micropollutants from water by ion-exchange polymers–effects of competing electrolytes, *Water Res.*, 2012, **46**, 5009–5018.

34 R. P. Schwarzenbach, P. M. Gschwend and D. M. Imboden, *Environmental Organic Chemistry*, John Wiley & Sons, 2016.

35 L. Konermann, Addressing a common misconception: ammonium acetate as neutral pH "buffer" for native electrospray mass spectrometry, *J. Am. Soc. Mass Spectrom.*, 2017, **28**, 1827–1835.

36 B. Bhhatarai and P. Gramatica, Prediction of aqueous solubility, vapor pressure and critical micelle concentration for aquatic partitioning of perfluorinated chemicals, *Environ. Sci. Technol.*, 2011, **45**, 8120–8128.

37 F. Xiao, X. Zhang, L. Penn, J. S. Gulliver and M. F. Simcik, Effects of monovalent cations on the competitive adsorption of perfluoroalkyl acids by kaolinite: experimental studies and modeling, *Environ. Sci. Technol.*, 2011, **45**, 10028–10035.

38 H. P. H. Arp, C. Niederer and K. Goss, Predicting the partitioning behavior of various highly fluorinated compounds, *Environ. Sci. Technol.*, 2006, **40**, 7298–7304.

39 P. Jing, P. J. Rodgers and S. Amemiya, High lipophilicity of perfluoroalkyl carboxylate and sulfonate: Implications for their membrane permeability, *J. Am. Chem. Soc.*, 2009, **131**, 2290–2296.

40 J. L. Guelfo and C. P. Higgins, Subsurface transport potential of perfluoroalkyl acids at aqueous film-forming foam (AFFF)-impacted sites, *Environ. Sci. Technol.*, 2013, **47**, 4164–4171.

41 C. Zhang, H. Yan, F. Li, X. Hu and Q. Zhou, Sorption of short- and long-chain perfluoroalkyl surfactants on sewage sludges, *J. Hazard. Mater.*, 2013, **260**, 689–699.

42 L. Xiang, T. Xiao, P. Yu, H. Zhao, C. Mo, Y. Li, H. Li, Q. Cai, D. Zhou and M. Wong, Mechanism and implication of the sorption of perfluorooctanoic acid by varying soil size fractions, *J. Agric. Food Chem.*, 2018, **66**, 11569–11579.